We are IntechOpen, the world's leading publisher of Open Access books Built by scientists, for scientists

4,800
Open access books available

122,000
International authors and editors

135M
Downloads

Our authors are among the

154
Countries delivered to

TOP 1%
most cited scientists

12.2%
Contributors from top 500 universities

WEB OF SCIENCE™

Selection of our books indexed in the Book Citation Index in Web of Science™ Core Collection (BKCI)

Interested in publishing with us?
Contact book.department@intechopen.com

Numbers displayed above are based on latest data collected.
For more information visit www.intechopen.com

19

Optical Deposition of Carbon Nanotubes for Fiber-based Device Fabrication

Ken Kashiwagi and Shinji Yamashita
Department of Electronic Engineering, The University of Tokyo
Japan

1. Introduction

Since carbon nanotubes (CNTs) have been applied to a passive mode-locker, or a saturable absorber (Set et al., 2004a; Set et al., 2004b), applications of CNTs in photonics field have been intensively investigated. Their quasi-one-dimensional structures produce their distinctive characteristics, their strong third-order nonlinearity and ultrafast recovery time, shorter than 1ps (Chen et al., 2002; Ichida et al., 2002). These characteristics are attractive for future ultrafast photonic networks and can be used in ultrafast photonic devices, such as ultrafast all-optical switches and all-optical logic gates.

Since CNTs are nano-sized material, one of the largest problems to realize CNT-based devices is handling issue. Optical deposition method has an advantage in efficiency over the other handling methods, such as spraying (Set et al., 2004a; Set et al., 2004b), direct synthesis (Yamashita et al., 2004), and polymer embedding methods (Sakakibara et al., 2005). These methods mostly require complicated processes, large-scale setups, and dissipate significant numbers of CNTs. A simpler and more cost effective handling technique of CNTs is required for mass productive CNT-based optical devices. We proposed optical CNT deposition technique to solve the problem. The light injection into CNT-dispersed solution from an optical fiber end deposited CNTs onto core region of the optical fiber end. We realized a passively mode-locked fiber laser using the CNT-deposited fiber as a saturable absorber, or a passive mode-locker.

However, the technique requires very precise control of the light injection power to deposit uniform and less scattering CNT layer, because highly uniform CNT solution, which has very small CNT entanglements, is required. Smaller CNT entanglements require higher injection power. High power injection makes the CNT layer around the core, not on the core. The upper limit of optical intensity depends on the flow speed caused by the injected light. Additional technique is, accordingly, needed to optimize injection power for each solution. We introduced in-situ optical reflectometry to monitor the deposition process, and area-selectively deposited CNTs onto core regions of optical fiber ends. The area-selectivity was confirmed by field emission scanning electron microscope (FE-SEM).

The technique has been applied only to deposition of CNTs onto fiber ends, though it has potentially versatile applications. We propose and demonstrate optically induced deposition of CNTs around microfibers by injecting light through the fibers. We also demonstrate a passively mode-locked fiber laser using a CNT-deposited microfiber fabricated by the technique.

Source: Frontiers in Guided Wave Optics and Optoelectronics, Book edited by: Bishnu Pal,
ISBN 978-953-7619-82-4, pp. 674, February 2010, INTECH, Croatia, downloaded from SCIYO.COM

In this chapter, we report optical deposition of CNTs onto optical fibers to realize simple and low cost fabrication of CNT-based fiber-structure devices. This chapter is organized as follows. In section 2, we explain CNT-based optical devices, including fundamental properties of CNTs, CNT fabirication methods, and structures of CNT-based optical devices. We propose the technique to deposit CNTs using light injection in section 3. In section 4, we show the technique with optical reflectometry to enhance the performance of the technique in terms of CNT-use efficiency and repeatability. We report application of the technique to CNT deposition around microfibers in section 5. Finally, we summarize this chapter in section 6.

2. Optical device based on carbon nanotubes

2.1 Carbon nanotubes fabrication methods

Graphite and diamond have been well known allotropes of carbon. In 1985, the third allotrope of carbon, fullerene, was discovered by Kroto et al. (Kroto et al., 1985), and carbon based nanomaterial research field emerged. CNTs are the forth new group of carbon materials which have nearly identical one-dimensional cylindrical structures, and their structures are assumed to be rolled sp^2-bonded graphene sheets. Graphene sheet is a sheet which carbon atoms are hexagonally bonding with each other. Since the discovery of CNTs by Iijima in 1991 (Iijima, 1991), theoretical studies of CNTs have been intensively examined. The studies brought out the distinctive physical properties of CNTs, such as their electronic density of states (eDOS), and metallic and semiconducting distinction that depends only on their structure, chirality (Saito et al., 1992). There are two types of CNTs in terms of their structures, single walled nanotubes (SWNTs) have only single cylinder, and multi walled nanotubes (MWNTs) have two or more cylinders. The CNTs which have optically interesting properties are the SWNTs.

Experimental studies on CNTs became possible after the establishment of production methods in the late 1990s, such as laser-furnace (Guo et al., 1995), arc-discharge (Journet et al., 1997), and catalytic CVD methods with supported catalysts (Dai et al., 1996) and floated catalysts (Satishkumar et al., 1998). These methods are used in the mass synthesis of CNTs in which the CNTs are obtained as soot adhered on the wall of the production chambers. Since the as-synthesized soot contains amorphous carbons, multi-shelled graphites, fullerenes, and/or catalyst metal particles as impurities, a purification process is generally required prior to use (Bandow et al., 1998; Bai et al., 2004; Chiang et al., 2001; Colomer et al., 1999; Morishita & Takarada, 1999; Park et al., 2006). The high pressure carbon mono-oxide (HiPco) method (Nikolaev et al., 1999) has been one of the commercialized fabrication methods for the mass production of CNTs.

The development of production methods of CNTs enabled experimental studies for specific applications. One of the applications is saturable absorbers for ultrashort pulse generation.

2.2 Optical characteristics of carbon nanotubes

In the previous subsection, we reviewed fabrication methods of CNTs. In this subsection, we briefly explain characteristics of CNTs, especially optical characteristics.

CNTs typically have 0.6 ~ 2 nm diameter and 1 μm length so that they have nearly identical 1D structures. CNT structures and their physical properties are determined by their diameter and chiral angle (rolling direction of graphene sheet). Fig. 1 shows an unrolled hexagonal lattice of a CNT, a graphene sheet. The chiral vector ($\boldsymbol{C}_h$) connects the two points

which become the identical point when we roll up the sheet to make it a cylinder, or a CNT. The vector is called the "chiral vector".

The chiral vector ($\boldsymbol{C}_h$) is expressed using unit vectors $\boldsymbol{a}_1$ and $\boldsymbol{a}_2$ and two integers n and m ($0 \le m \le n$) as

$$\mathbf{C}_h = n\mathbf{a}_1 + m\mathbf{a}_2 \equiv (n,m) \tag{1}$$

The type of CNT is completely determined by the two integers (n,m) through the definition given in Eq. (1). For example, (6,2) chiral vector is shown in Fig. 1. Originating from their 1D structure, wave vectors of CNTs are discretely existing. This discretion form a sharp divergence in their electron density of state (eDOS), called "van Hove singularities," that is typical characteristic of 1D materials.

Their eDOS structures are determined by their chirality. We can classify CNTs into two groups, metallic and semiconducting. In general, mod($n-m$, 3) = 0 CNTs are metallic and mod($n-m$, 3) ≠ 0 CNTs are semiconducting. One of the most important characteristics of CNTs is that the difference between metallic and semiconducting properties is determined by their chirality.

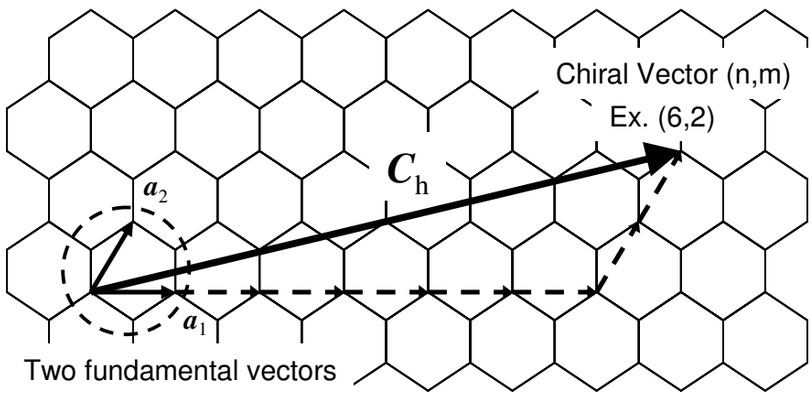

Fig. 1. Schematics of 2D graphene sheet

Semiconducting CNTs absorb the light whose energies are same as their bandgaps. The bandgap energies are controllable by choosing appropriate CNTs diameter, since the bandgap energies are almost inversely proportional to their diameters. The CNTs work as saturable absorbers in the absorption band. Saturable absorbers are materials or devices which change their absorbance depends on power of incident light. They absorb the light which has low intensity, whereas the absorbance decreases due to the saturation of absorption in the case of high intensity light. This phenomenon can be understood as eDOS occupation in conduction bands of saturable absorber material (Fig. 2). If the low intensity light incidents, electrons in valence band are excited up to conduction band, and photons are highly absorbed. On the other hand, if the optical intensity is high, some photons are not absorbed because the eDOS in conduction band is occupied with other electrons which excited by the light. Thus, the optical intensity dependent transparency, the saturable absorption reveals.

This kind of intensity dependent attenuation enables the high-intensity components of an optical pulse to pass through saturable absorbers, while the lower intensity components of the pulse, such as the pulse wings, pedestals, and background CW radiation, not to pass

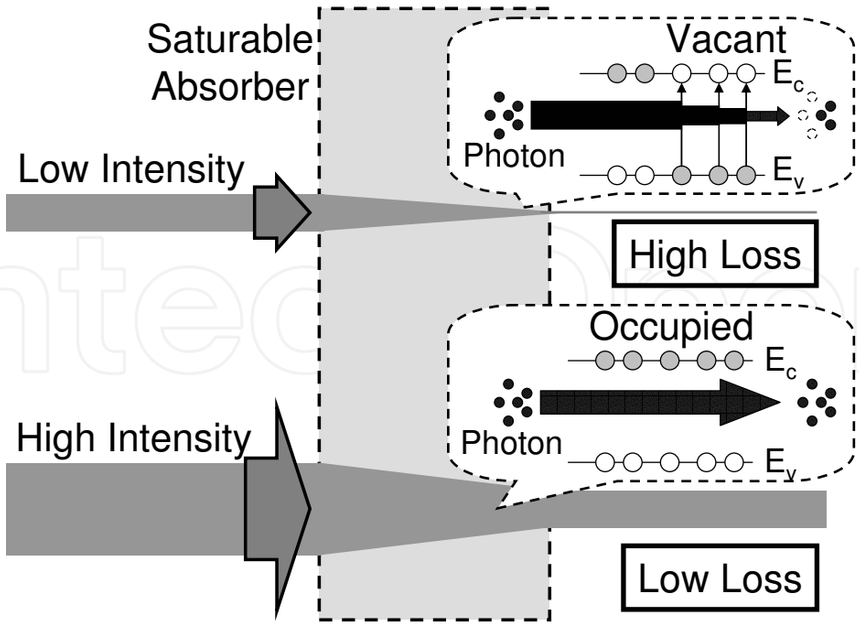

Fig. 2. Schematics of saturable absorption (E_v and E_c denotes energy levels of valence band and conduction band, respectively)

(Fig. 3). When a saturable absorber is inserted in a laser cavity, amplified spontaneous emission (ASE) noise of a gain medium is shaped to be a pulse train. In every round trip, light pass the saturable absorber as high intensity noise with low loss and low intensity noise with high loss, resulting in high intensity contrast. Finally, light start to oscillate in pulsed state.

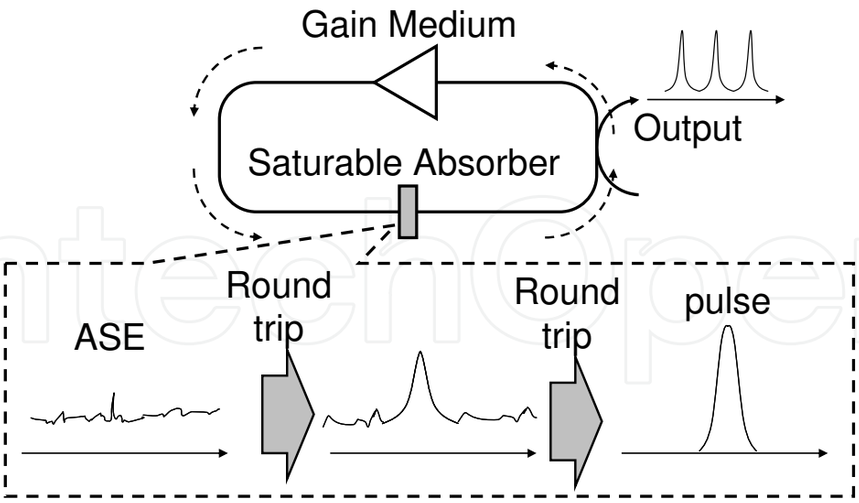

Fig. 3. Schematics of noise suppression by saturable absorber

For ultrashort pulse generation, a saturable absorber with a fast recovery time is required for stabilizing laser mode-locking, while a slower recovery time could facilitate laser self-starting. Recovery time of CNTs have been measured to be shorter than 1 ps, and CNTs are suitable material for ultrashort pulse generation. However, the recovery time of CNTs only

consisted by semiconducting CNTs is not so fast (around 30 ps) (Rubtsov et al., 2004). The ultrafast response time of CNTs are based on bundles and/or entanglements of semiconducting and metallic CNTs because the electrons which are excited by photons in semiconducting CNTs couple to metallic CNTs, resulting in ultrafast recovery time of semiconducting CNTs. As-synthesized CNT samples consist of CNTs which have several different chiralities, including both metallic and semiconducting CNTs. Therefore, the CNT samples inherently have ultrafast recovery time shorter than 1 ps.

It is difficult to selectively fabricate CNTs which have certain chirality. However, the mixture of several types of CNTs have two advantages. One of the advantages is ultrashort recovery time which we mentioned above. Another advantage is its wide absorption band. Different chiralities of CNTs have different absorption band, and, consequently, their mixture effectively has very wide absorption band. The wide saturable absorption band is required for passively mode-locked laser whose output pulse width is ultrashort, such as femtosecond regime.

2.3 CNT based optical device structures and fabrication methods

After CNT optical devices were first demonstrated, three types of CNTs based device structures have been proposed. They are depicted in Fig. 4, transmission type, reflection type and fiber end type. These device structures were confirmed to have good performance to provide CNT-based optical devices. However, the fabrication process had some problems in terms of efficiency.

The three types of devices was first fabricated and demonstrated by spraying method (Set et al., 2004a; Set et al., 2004b). The spraying method is common method to evaluate and characterize CNT samples. In the method, we first prepare a CNT-dispersed solution. CNTs tend to be entangled with each other, and few kinds of solvents can be used to disperse them in high uniformity and fewer entanglements. DMF is one of the most commonly used solvents where CNTs can be dispersed. After the preparation, we spray substrates and fiber ends with the solution, and evaporate the residual DMF by heat. The largest advantage of this method is simplicity: we can fabricate optical devices using simple setup. However, the efficiency of CNT-use is poor. The sprayed solution spread around the target position where we want to deposit CNTs.

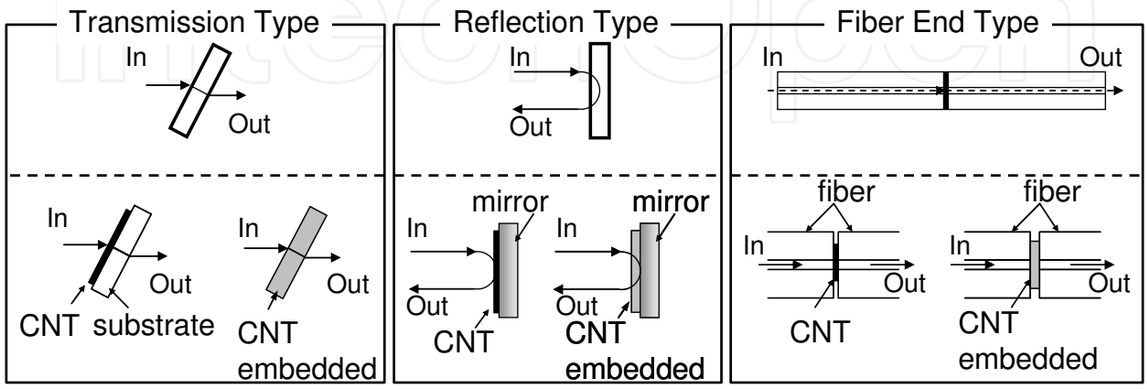

Fig. 4. Schematics of three types of carbon nanotubes optical devices

After the proposal, direct synthesis method (Yamashita et al., 2004) and polymer embedding method (Sakakibara et al., 2005) have been reported. Though embedding CNTs into polymer materials have been already demonstrated (Sakakibara et al., 2003), the report was the first application to the passive mode-locker in the fiber-end-type configuration. The polymer embedding method can remove the impurities before embedding CNTs into polymer materials. The method requires setups for polymer material processing, and the large number of CNTs is not settled through optical pass of devices. In the direct synthesis method, CNTs were directly synthesized onto optical fiber ends, and the fiber produced passively mode-locking of a fiber laser. However, there is no method to remove impurities in as-synthesized CNTs, and consequently ultra-high performance CNT fabrication setup is required.
From the next section, we show our proposal of optical deposition of CNTs. Our proposal offers very simple CNT-based optical device fabrication method, and efficiency of CNT-use drastically increases.

3. Optical deposition of carbon nanotubes

3.1 Optical deposition of carbon nanotubes onto fiber ends

There is a problem in handling CNTs because CNTs tend to entangle with each other and they are difficult to be dispersed in common solvents. In optical device applications, CNTs are conventionally used by spraying, directly synthesizing onto a device, or embedding into a polymer material. These processes are mostly complicated, large-scale setups are required and CNTs are not efficiently used in these methods. To minimize the dissipation number of CNTs, we have proposed and demonstrated optical deposition of CNTs. The method enables area-selective deposition of CNTs only onto a core region of an optical fiber end. This technique will drastically improve the efficiency of CNT usage and the fabrication costs of CNT-based photonic devices.
Our experimental setup is very simple as shown in Fig. 5. It is composed of just two equipments, a laser diode and an erbium doped fiber amplifier (EDFA). We first prepared a purified CNT-dispersed DMF solution. Light produced from a laser diode which had the wavelength of 1560 nm and the optical power of -10 dBm was amplified upto about 20 dBm by a high-power EDFA. The light was incident into the solution through a cleaved fiber end. We observed CNT deposition conditions on the fiber end facets using a microscope for several different optical powers. Microscopic Raman spectroscopy was used to confirm the existence of CNTs at selected area. To find the dependence of the numerical aperture (NA) of the optical fiber, we used two types of optical fibers having different NAs, single-mode fibers (SMFs) and dispersion-shifted fibers (DSFs).

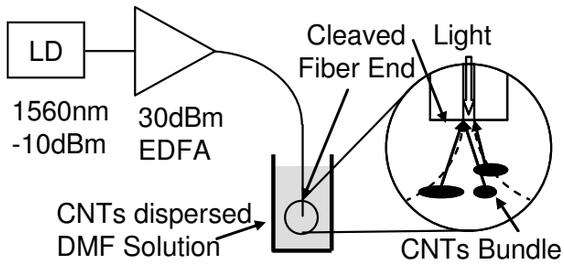

Fig. 5. Experimental setup for optically depositing carbon nanotubes onto fiber end

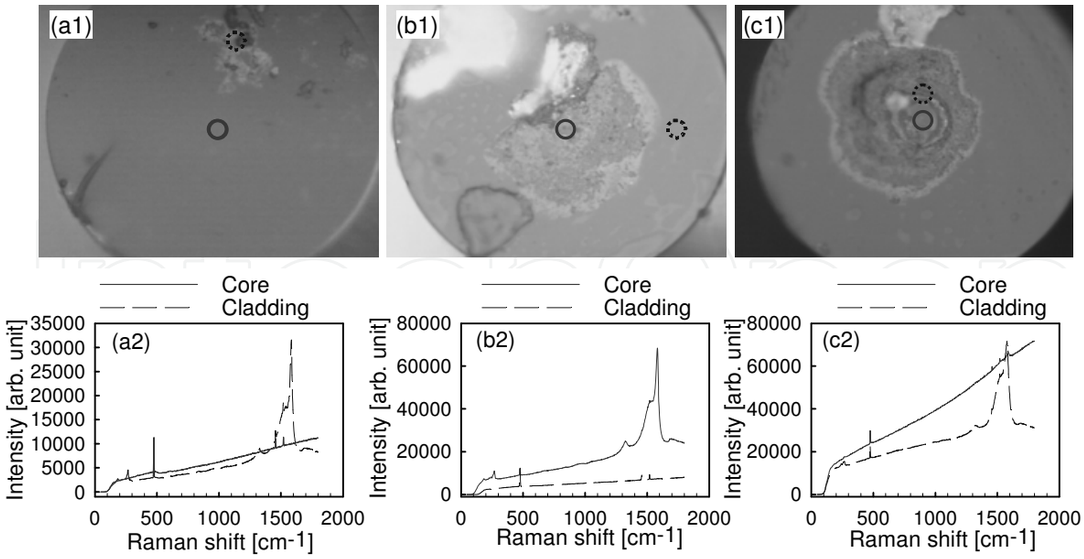

Fig. 6. Microscope images and Raman spectra of CNT-deposited SMF ends. Injected light power: (a) 20.0, (b) 21.5, and (c) 22.0 dBm.

In Fig. 6, microscope images and Raman spectra of CNTs deposited fiber ends of standard SMFs are shown. Fig. 6 (a), (b), (c) correspond to incident optical power of 20 dBm, 21.5 dBm and 22.0 dBm, respectively. Solid circles in Fig. 6 (a1), (b1), (c1) indicate core areas of SMFs, and corresponding Raman spectra are shown with solid curves in Fig. 6 (a2), (b2), (c2). Broken circles are the areas where CNTs are deposited outside of the core, and corresponding Raman spectra are shown with broken curves.

There are three major peaks in the Raman spectra of CNTs. The most typical peak of CNT appears at around 250 cm^{-1}, and it due to the radial breathing mode (RBM), which is a vibration mode of CNTs in the radial direction. We confirmed the presence of CNTs from the peak. The optical power of 20.0 dBm was not enough to trap the CNTs, whereas Fig. 6 (a) shows the existence of CNTs that may be accordingly attached to the cladding region of the fiber end. In Fig. 6 (b), CNTs were area-selectively deposited onto the fiber end only on the core region, and the Raman spectrum shows the existence of CNTs. By increasing the optical power up to 22.0 dBm, CNTs were not deposited onto the core region but deposited around the core.

In the case of DSF, an optical power of 19.0 dBm was enough to deposit CNTs. Fig. 7 shows a microscope image of the fiber end facet and its Raman spectrum at the core center. By increasing the optical power up to 21.5 dBm, CNTs were deposited around the core. Stronger confinement of light in DSF reduced the required optical power for CNT deposition by 2.5 dB, and widened the margin to ±2 dB.

The principle of this technique is not yet confirmed, but we presume that one possible mechanism is the optical tweezer effect, which is caused by the optical intensity diversion of the light in a solution. Another possible mechanism would be the flow of solution due to the injected light. The light might thermally induce convection and swirl nearby the core, and entangled CNTs were attached.

It is possible to deposit CNTs onto a fiber ferrule end as shown in Fig. 8. We deposited CNTs onto an end facet of a standard SMF with a ferrule using an optical intensity of 21.5

dBm, which is the same experimental condition as that of the fiber shown in Fig. 6 (b). Raman spectra in Fig. 8 show that CNTs were area selectively deposited only onto the core region. This technique will reduce the alignment cost after CNT deposition.

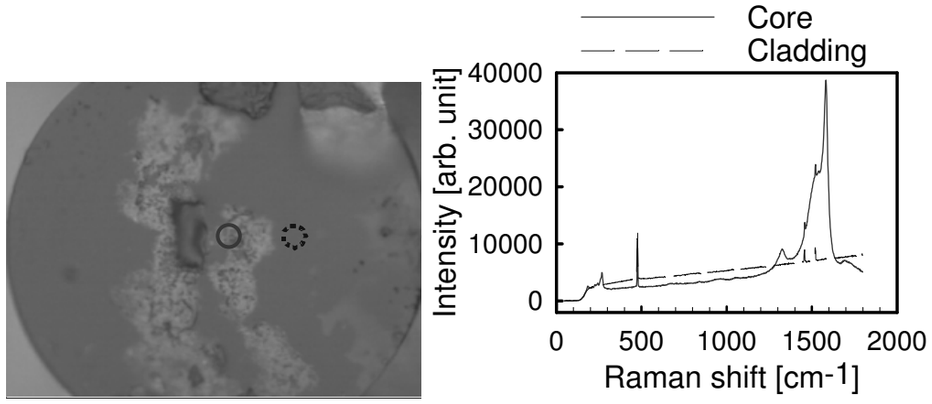

Fig. 7. Microscope image and Raman spectrum of CNTs deposited onto DSF end using 19.0 dBm injected light.

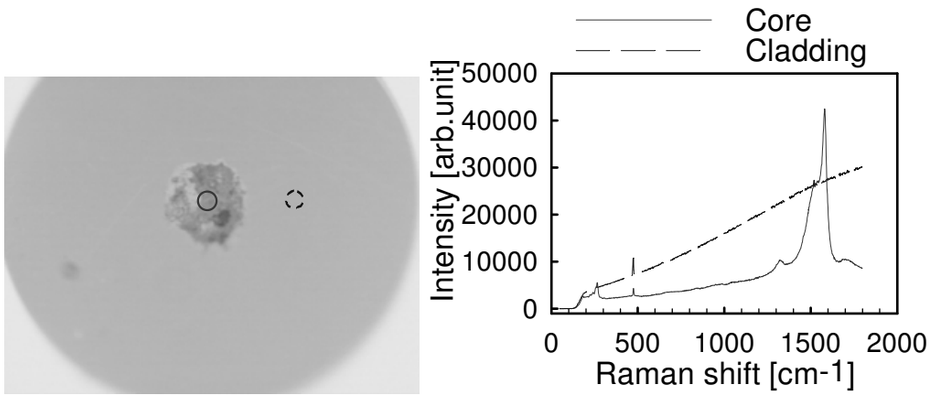

Fig. 8. Microscope image and Raman spectrum of CNT-deposited SMF end with ferrule using 21.5 dBm injection light.

3.2 Passive mode locking of fiber laser using optically deposited CNTs

In previous subsection, we have explained the method to deposit CNTs only onto the core region of optical fiber ends. We have deposited CNTs onto optical fiber end with ferrule intended to use as a saturable absorber. In this subsection, to ensure that the performance of the technique is sufficient for fabricating optical devices, we report a passively mode-locked fiber laser that employs the fiber, which had optically deposited CNTs on its fiber end.

The experimental setup is shown in Fig. 9. An EDFA was used as the laser gain medium and an isolator was inserted to prevent back reflection in the cavity to ensure one-directional lasing. We controlled the polarization state using a polarization controller (PC). The total dispersion in the laser cavity was adjusted to be nearly zero by inserting a 20-m-long SMF. The output light came out from a 3 dB coupler. A CNT-deposited fiber on its end with ferrule was inserted as an alignment-free passive mode-locker. The insertion loss of the fiber was about 4.2 dB. We measured an optical spectrum using an optical spectrum analyzer and an autocorrelation trace using a second-harmonic generation (SHG) autocorrelator.

By injecting 200 mA to the pump laser of the EDFA and controlling the polarization state of the light inside the laser cavity, we achieved passively mode-locked oscillation. An optical spectrum of the laser output measured with a 0.1 nm resolution is shown in Fig. 10 (a). The 3 dB spectral width was 3.2 nm. The SHG autocorrelation trace with a 50 fs resolution is shown in Fig. 10 (b) and had a full-width at half-maximum (FWHM) of 630 fs. Assuming a transform-limited sech² pulse waveform, the pulse width is calculated to be as short as 400 fs. The pulse width was almost independent of EDFA gain and was highly dependent on the dispersion of the laser cavity.

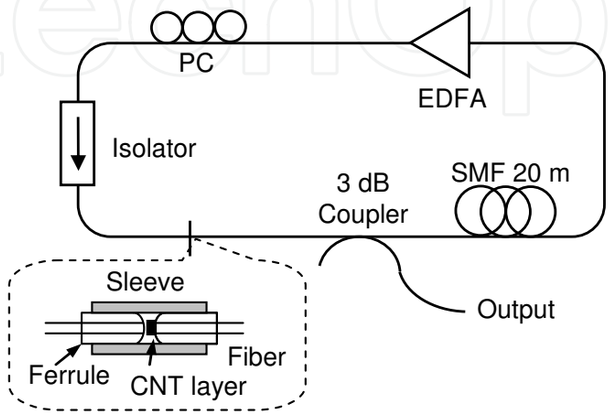

Fig. 9. Experimental setup for passively mode-locked fiber laser using a CNT-deposited fiber as a saturable absorber.

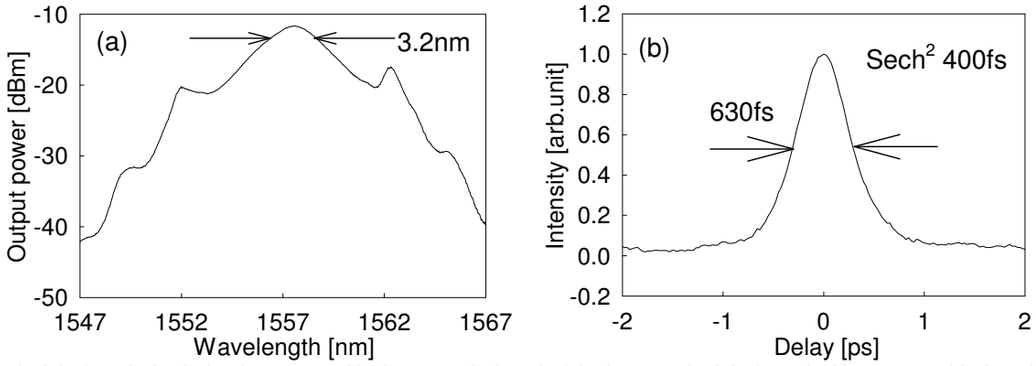

Fig. 10. Optical output characteristics of passively mode-locked fiber laser in Fig. 9 (a) Optical spectrum (resolution 0.1 nm). (b) SHG autocorrelation trace (resolution 50 fs).

4. In-situ monitoring of optical deposition of carbon nanotubes onto fiber end

The method described in the previous section requires only a lightsource to deposit CNTs onto a core region of an optical fiber end. Light injection from the fiber end into CNT-dispersed solution preferentially deposits CNTs onto core regions of optical fiber ends, resulting in efficient CNT-use. Optical pass alignment, therefore, is not necessary for this technique.

However, the technique requires very precise control of the light injection power to deposit uniform and less scattering CNT layer because highly uniform CNT solution, which has

very small CNT entanglements, is required. Smaller CNT entanglements require higher injection power. With the increase of the light intensity, flow induced by the light injection becomes too high speed to trap the CNTs onto the core. High power injection deposits CNTs around the core, not on the core, as we have already depicted in Fig. 6. The upper limit of optical intensity depends on the flow speed caused by the injected light. Additional technique is, accordingly, needed to optimize injection power for each solution. In this section, we employed optical reflectometry to simplify the optimization process and deposit CNTs onto very small areas.

The experimental setup for the in-situ optical reflectometry is shown in Fig. 11. Light at a wavelength of 1560 nm from a laser diode was used for both the optical deposition and the optical reflectometry. The light was amplified by a high-power EDFA, and subsequently was split into two by a 10:90 coupler. The 10 % of the light was monitored for reference by a power meter after 20 dB attenuation. The light of 90 % was injected from a cleaved fiber end into a DMF solution, where purified CNTs were uniformly dispersed. The power of the reflected light from the fiber end was measured by another power meter through a circulator. The reference and the reflected light powers were measured at every 500 msec. The refractive indices of DMF and silica-glass are 1.42 and 1.44, respectively. Since the refractive index difference between DMF and silica-glass was small, the reflection was suppressed before CNT deposition. On the contrary, semiconducting CNTs had the refractive indecies of around 3.0, though the refractive indecies of CNTs depend on their chiralities(Margulis & Gaiduk, 2001).

The reflectivity drastically increased after the first deposition of an entanglement. The deposition was achieved by the optimization of the injection power with monitoring the reflection. Even if we repeat the experiment by changing the injection power with the highly uniform CNT solution, we could not deposit the CNTs only onto the core without the reflectometry. It was because there was very small margin of the injection power when we used the highly uniform CNT solution. Moreover, the solution condition, especially the sizes of the CNT bundles, changed in time and this prevented us from the preferential deposition without the reflectoemtry. The optical reflectometry offered the detection capability of the starting time of CNT deposition to the system and, consequently, controllability of the number of CNTs by adjusting the light injection duration after the deposition started. Subsequent to the process, we took microscope images and field emission scanning electron microscope (FE-SEM) images of the fiber ends.

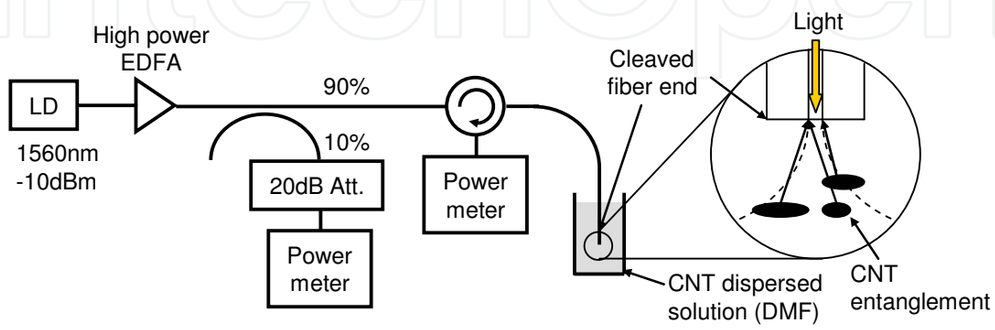

Fig. 11. Experimental setup for optically manipulated CNT deposition with optical reflectometry monitoring.

Fig. 12 shows in-situ optical reflectometry data series which describe the deposition processes of thin and thick layers. Once the EDFA was turned on, its output was kept constant around at 20 dBm. It took a short period of time (10 - 100 s) to start the deposition. The start times were not the same in the two cases because the solution was not completely uniform. The reflectivity was as small as -40 dB because of the small refractive index difference between DMF and the fiber. Fig. 12 clearly show the drastic increase of the reflectivities about 20 dB due to the first entanglement deposition. The thicknesses were controlled by changing the light injection period after the increase of reflectivity. To deposit a thin layer, the EDFA was turned off at 8 seconds after the start of deposition as shown in Fig. 12 (a). In the case of the thick layer deposition, the EDFA kept on for about 4 minutes after the deposition starting. During the deposition, the fluctuation of reflectivity gradually decreased (Fig. 12 (b)). It indicates that the CNT layer gradually became uniform.

The introduction of optical reflectometry produced important functionalities to the system: deposition starting time detection and in-situ layer uniformity evaluation. The thickness of CNT layer could be roughly adjusted by controlling duration of injection even without the reflectometry. Since entangled CNTs which flowed to a fiber end were trapped and deposited, CNT deposition did not start just after the light injection. This was the reason why it was difficult to control the number of CNTs. First deposition of CNT entanglement drastically increased reflectivity at the fiber end due to the high index contrast between CNTs and silica-glass. It, then, became a seed of a CNT layer and the deposition continued because of strong Van der Waals force among CNTs. The duration of the deposition, therefore, controlled the layer thickness by introducing optical reflectometry. As the layer became more uniform, the reflection became less affected by the solution flow. The fluctuation of the reflectivity gradually decreased.

Optical microscope images of the thin and thick layers are shown in Fig. 13. The figures describe the thickness difference between the two layers. To directly observe the existence of CNTs, the layer thicknesses and the sizes of the deposition regions, we took the FE-SEM images of the fiber ends shown in Fig. 14 and Fig. 15. The thin CNT layer was clearly observed only at the core region in Fig. 14, whereas the deposited layer was very thick in Fig. 15. The thick layer was preferentially deposited only onto ~15 μm diameter circular region. This result was achieved using the highly uniform solution solution and the precise optimization of injection power which was enabled by the in-situ optical reflectometry.

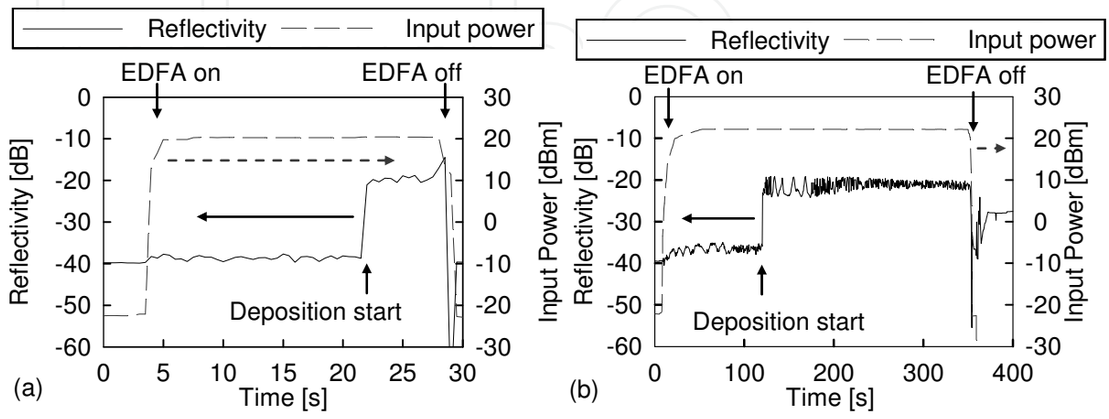

Fig. 12. Data series of optical reflectometry of CNT deposition (a)thin layer deposition process (b)thick layer deposition process.

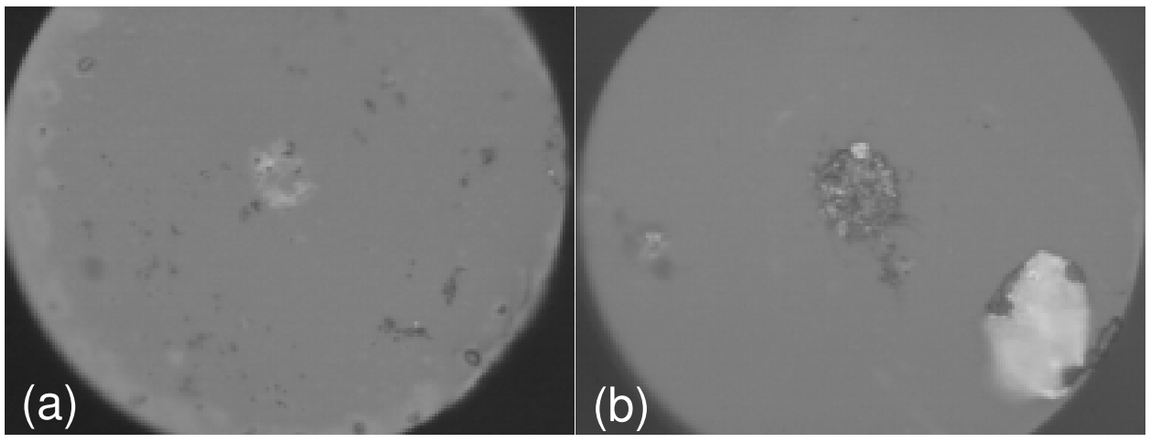

Fig. 13. Optical microscope images of fiber ends with CNT layers on the core region (a) thin CNT layer (b) thick CNT layer.

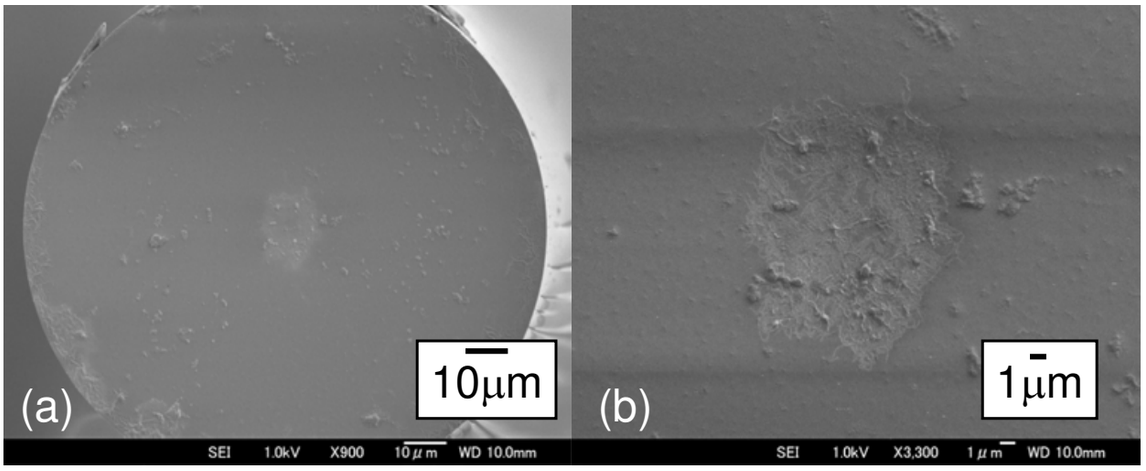

Fig. 14. FE-SEM images of the fiber end with the thin layer (a) whole fiber end (b) magnified around the core region

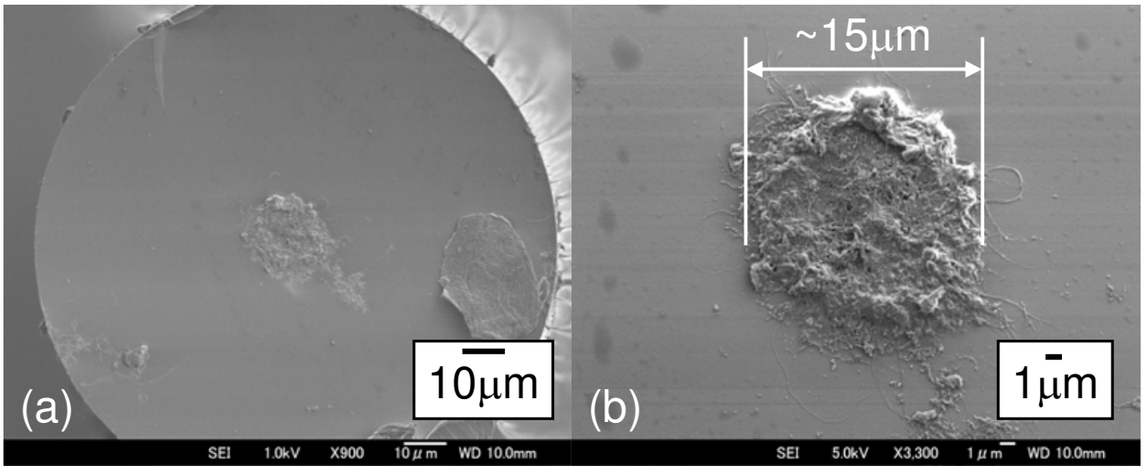

Fig. 15. FE-SEM images of the fiber end with the thick layer (a) whole fiber end (b) magnified around the core region.

5. Optical deposition of CNTs around microfiber

In section 3 and 4, we reported the optical deposition of CNTs onto the optical fiber ends. In this section, we show one aspect of versatility of the deposition method, CNT deposition around a microfiber. Evanescent coupling between CNTs and propagation mode of a microfiber is one way to realize polarization insensitve CNT device as already reported (Kieu & Mansuripur, 2007; Song et al., 2007).

First, we fabricated a microfiber using an experimental setup shown in Fig. 16. A bare standard single mode fiber (SMF) was set on two fiber holders, which were fixed on two translation stages. The fiber ends were connected to an erbium doped fiber amplifier (EDFA) and a power meter, respectively. We fabricated a microfiber by stretching the fiber with heat produced by a flame. During the fabrication process, we monitored the insertion loss of the fiber using the power meter. The fiber was tapered down so that its taper waist diameter became ~6 μm.

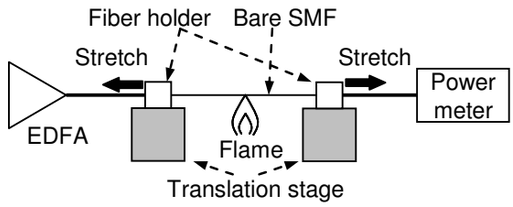

Fig. 16. Schematic of fabrication of microfiber

Next, we deposited CNTs around the microfiber using a setup shown in Fig. 17. The fabricated microfiber was immersed into a CNT-dispersed DMF droplet on a slide glass. Light from a laser diode at a wavelength of 1560 nm and at -10 dBm optical power was amplified up to 13 dBm by an EDFA and consequently injected into the microfiber. The output power was monitored by a power meter to detect start of CNT deposition, and consequently to control the deposition time.

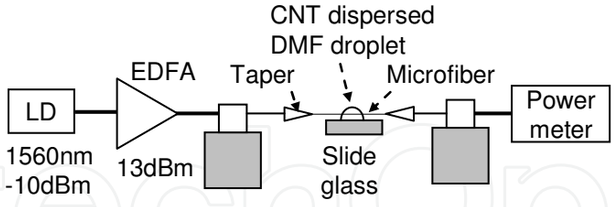

Fig. 17. Schematic of optical deposition of CNT around microfiber

Fig. 18 (a) shows a microscope image of a CNT-deposited microfiber, whose waist diameter was ~6 μm. We found that the CNTs start to be deposited around the microfiber at the incident power of 13 dBm. To ensure the existence of CNTs, we performed microscopic Raman spectroscopy. The dotted circle in Fig. 18 (a) was the area where microscopic Raman spectroscopy was performed. The microscopic Raman spectrum in Fig. 18 (b) confirms that the CNTs were certainly deposited around the microfiber. The optical deposition technique was confirmed to be applicable not only to deposition onto fiber ends but also to deposition around microfibers. We could detect the start of the CNT deposition by the drop of the output power due to scattering and absorption induced by deposited CNTs. We stopped the light injection about 5 sec after the deposition started. The excess loss induced by the tapering was 0.2 dB. The CNT deposition increased insertion loss by 5.8 dB and the total loss was 6 dB.

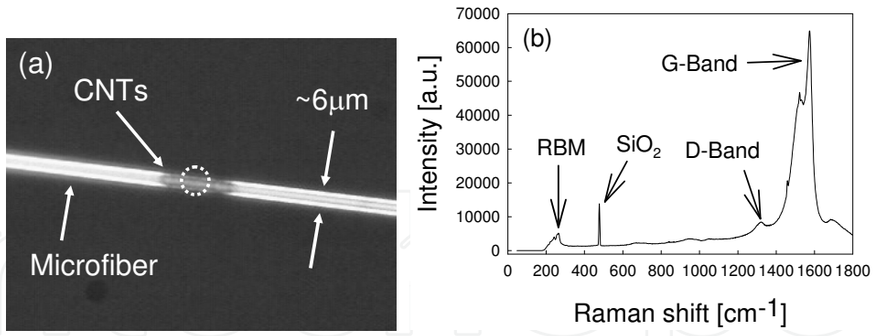

Fig. 18. (a) Microscope image of CNT-deposited microfiber (waist ~6 μm), dotted circle indicates area where microscopic Raman spectrum was measured, (b) Microscopic Raman spectrum of CNT-deposited microfiber.

We presume the similar phenomenon occurred both in the case of optical CNT deposition onto fiber ends and around microfibers. In the case of the CNT deposition onto fiber ends, swirl and convection caused by the light injection to a CNT-dispersed solution might deposit CNTs. The deposition mechanism might be the combination of the convection and the optical tweezer effect. On the contrary, in the present experiment, the light injection from air into the droplet thermally caused swirl and convection at the boundary. The swirl and convection induced by the light injection might deposit the CNTs around the microfibers. This phenomenon occurs only at the light input side boundary, and enables us to area-selectively deposit them onto desired position. Another possible mechanism is the optical tweezer effect, which can traps micro- and nano-sized objects by the optical intensity diversion in the solution. Evanescent field had the optical intensity diversion, and mode field mismatch between the air section and the DMF section caused the optical intensity diversion by scattering. The diversion might trap the CNTs and deposited onto the microfiber.

In order to confirm the saturable absorption property of the fabricated device, we applied it to mode-lock a fiber laser. We inserted the fiber, mentioned above, in a fiber laser cavity to achieve a passive mode-locking. The experimental setup is shown in Fig. 19. An EDFA produced gain of the laser. The polarization state inside the laser cavity was controlled by a polarization controller (PC). An isolator eliminated back-reflection inside the laser cavity, mainly occurred at the tapering region and the CNT-deposited part. The laser output came out from a 10% port of a 10:90 coupler. We measured optical spectrum and second harmonic generation (SHG) autocorrelation trace of the laser output using an optical spectrum analyzer and a SHG autocorrelator. We measured pulse repetition rate using a photodiode and an oscilloscope.

Fig. 20 shows an optical spectrum, an autocorrelation trace and a pulse train of the fiber laser output. The laser had the center wavelength at 1565 nm and the 3-dB bandwidth of 3.7 nm. The full width half maximum (FWHM) of the autocorrelation trace was 1.61 ps, which correspond to inferred pulse duration of 1.14 ps (assuming Gaussian pulse profile). The time bandwidth product (TBP) of the pulse was 0.528. Comparing to an unchirped transform-limited value of Gaussian pulse (0.441), the result indicates the pulse had chirp. The chirp was due to the residual dispersion in the laser cavity. The repetition rate of the fiber laser was 1.54 MHz according to the time interval of the output pulse train.

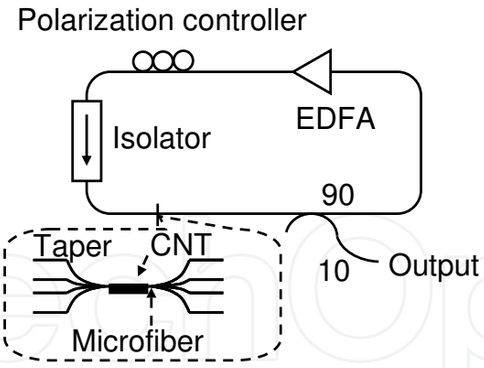

Fig. 19. Schematic of a passively mode-locked fiber laser using a CNT-deposited microfiber.

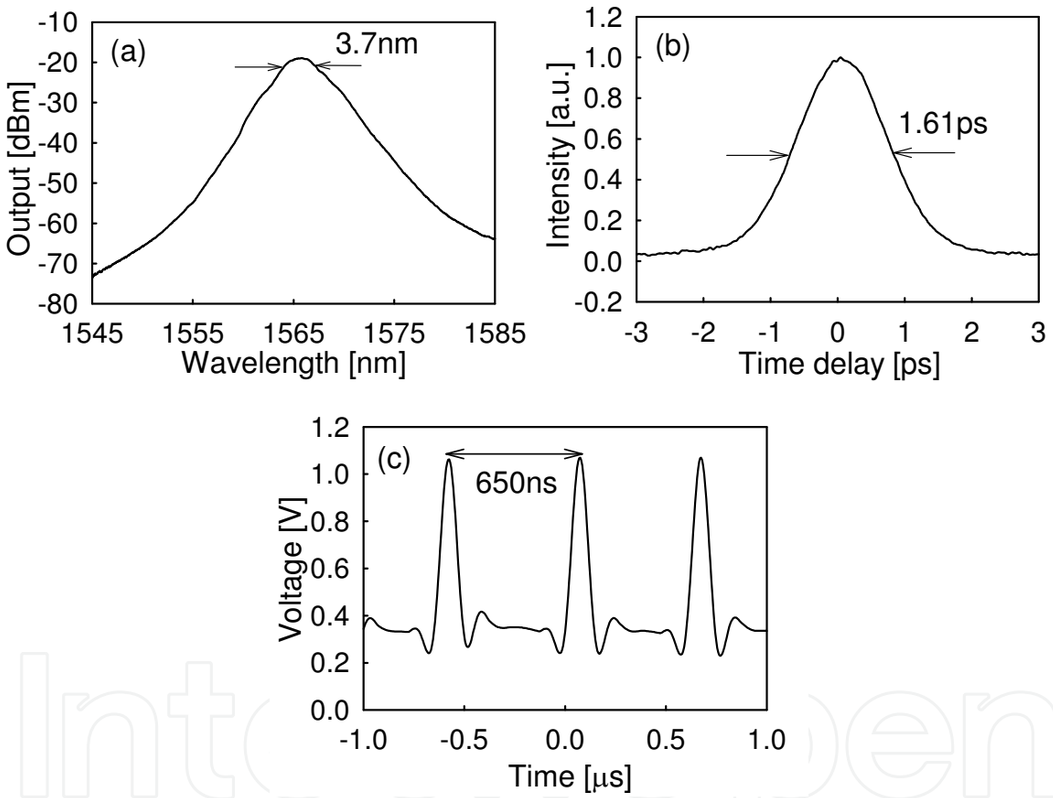

Fig. 20. Passively mode-locked fiber laser output (a) Optical spectrum of the fiber laser (resolution: 0.1 nm) (b) Autocorrelation trace of laser output (resolution: 50 fs,) corresponding pulse width: 1.14 ps (assuming Gaussian pulse) (c) Output pulse train of the fiber laser (repetition rate: 1.54 MHz)

6. Conclusion

In this chapter, we have proposed and demonstrated the optical deposition method of CNTs. After brief introduction of this chapter (section 1), we explained the general characteristics, optical properties, and optical devices based on CNTs in section 2. From

section 3, we reported optical deposition of CNTs. In section 3, we deposited CNTs by injected light from the optical fiber end into a CNT-dispersed solution. In subsection 3.1, we area-selectively deposited CNTs only onto the core region of optical fiber ends, such as a bare SMF and a bare DSF, by controlling the injection power. The area-selectivity was confirmed by microscopic Raman spectroscopy. A SMF with ferrule could be used as a deposition object, and it produced passive mode-locking of a fiber laser after the deposition (subsection 3.2).

The result confirmed the technique to have good performance of CNT-based device fabrication. However, the result showed that we need strict power control of the injection light within 2 dB for SMF. To solve this problem, we employed optical reflectometry into the method for in-situ monitoring of the deposition in section 4. The reflectometry offered easy optimization method for the injection power control. We deposited CNTs onto very small area (~15 μm diameter circular region) using highly uniform CNT-dispersed solution.

In section 5, we showed that the optical deposition method was also applicable to microfibers. We achieved CNT deposition around a microfiber, which were immersed in a CNT-dispersed DMF droplet, by injecting light through the microfiber. We confirmed the fiber could be used as a passive mode-locker in a fiber ring laser.

We believe our proposed method, optical deposition of CNTs, will contribute to development of ultrafast photonic applications based on CNTs in device fabrication aspect.

7. References

Bai et al., 2004. Bai, X., Li, D., Du, D., Zhang, H., Chen, L. & Liang, J. (2004), 'Laser irradiation for purification of aligned carbon nanotube films', *Carbon* 42(10), 2125 – 2127.

Bandow et al., 1998. Bandow, S., Asaka, S., Zhao, X. & Ando, Y. (1998), 'Purification and magnetic properties of carbon nanotubes', *Applied Physics A: Materials Science & Processing* 67(1), 23 – 27.

Chen et al., 2002. Chen, Y.-C., Raravikar, N., Schadler, L., Ajayan, P., Zhao, Y.-P., Lu, T.-M., Wang, G.-C. & Zhang, X.-C. (2002), 'Ultrafast optical switching properties of single-wall carbon nanotube polymer composites at 1.55 μm', *Applied Physics Letters* 81(6), 975–977.

Chiang et al., 2001. Chiang, I., Brinson, B., Huang, A., Willis, P., Bronikowski, M., Margrave, J., Smalley, R. & Hauge, R. (2001), 'Purification and characterization of single-wall carbon nanotubes (swnts) obtained from the gas-phase decomposition of co (hipco process)', *Journal of Physical Chemistry B* 105(35), 8297 – 8301.

Colomer et al., 1999. Colomer, J.-F., Piedigrosso, P., Fonseca, A. & Nagy, J. (1999), 'Different purification methods of carbon nanotubes produced by catalytic synthesis', *Synthetic Metals* 103(1-3 pt 3), 2482 – 2483.

Dai et al., 1996. Dai, H., Rinzler, A., Nikolaev, P., Thess, A., Colbert, D. & Smalley, R. (1996), 'Single-wall nanotubes produced by metal-catalyzed disproportionation of carbon monoxide', *Chemical Physics Letters* 260(3-4), 471 – 475.

Guo et al., 1995. Guo, T., Nikolaev, P., Thess, A., Colbert, D. & Smalley, R. (1995), 'Catalytic growth of single-walled nanotubes by laser vaporization', *Chemical Physics Letters* 243(1-2), 49 – 54.

Ichida et al., 2002. Ichida, M., Hamanaka, Y., Kataura, H., Achiba, Y. & Nakamura, A. (2002), 'Ultrafast relaxation dynamics of photoexcited states in semiconducting single-walled carbon nanotubes', *Physica B: Condensed Matter* 323(1-4), 237 – 238.

Iijima, 1991. Iijima, S. (1991), 'Helical microtubules of graphitic carbon', *Nature* 354(6348), 56–58.

Journet et al., 1997. Journet, C., Maser, W. K., Bernier, P., Loiseau, A., de la Chapelle, M. L., Lefrant, S., Deniard, P., Lee, R. & Fischer, J. E. (1997), 'Large-scale production of single-walled carbon nanotubes by the electric-arc technique', *Nature* 388(6644), 756–758.

Kieu & Mansuripur, 2007. Kieu, K. & Mansuripur, M. (2007), 'Femtosecond laser pulse generation with a fiber taper embedded in carbon nanotube/polymer composite', *Opt. Lett.* 32(15), 2242–2244.

Kroto et al., 1985. Kroto, H., Heath, J., O'Brien, S., Curl, R. & Smalley, R. (1985), 'C_{60}: Buckminsterfullerene', *Nature* 318(6042), 162–163.

Margulis & Gaiduk, 2001. Margulis, V. & Gaiduk, E. (2001), 'Nature of near-infrared absorption in single-wall carbon nanotubes', *Physics Letters A* 281(1), 52 – 58.

Morishita & Takarada, 1999. Morishita, K. & Takarada, T. (1999), 'Scanning electron microscope observation of the purification behaviour of carbon nanotubes', *Journal of Materials Science* 34(6), 1169 – 1174.

Nikolaev et al., 1999. Nikolaev, P., Bronikowski, M., Bradley, K., Rohmund, F., Colbert, D., Smith, K. & Smalley, R. (1999), 'Gas-phase catalytic growth of single-walled carbon nanotubes from carbon monoxide', *Chemical Physics Letters* 313(1-2), 91 – 97.

Park et al., 2006. Park, T.-J., Banerjee, S., Hemraj-Benny, T. & Wong, S. S. (2006), 'Purification strategies and purity visualization techniques for single-walled carbon nanotubes', *Journal of Materials Chemistry* 16(2), 141 – 154.

Rubtsov et al., 2004. Rubtsov, I., Russo, R., Albers, T., Deria, P., Luzzi, D. & Therien, M. (2004), 'Visible and near-infrared excited-state dynamics of single-walled carbon nanotubes', *Applied Physics A: Materials Science and Processing* 79(7), 1747 – 1751.

Saito et al., 1992. Saito, R., Fujita, M., Dresselhaus, G. & Dresselhaus, M. (1992), 'Electronic structure of chiral graphene tubules', *Applied Physics Letters* 60(18), 2204 – 2206.

Sakakibara et al., 2005. Sakakibara, Y., Rozhin, A. G., Kataura, H., Achiba, Y. & Tokumoto, M. (2005), 'Carbon nanotube-poly(vinylalcohol) nanocomposite film devices: Applications for femtosecond fiber laser mode lockers and optical amplifier noise suppressors', *Japanese Journal of Applied Physics, Part 1: Regular Papers and Short Notes and Review Papers* 44(4 A), 1621 – 1625.

Sakakibara et al., 2003. Sakakibara, Y., Tatsuura, S., Kataura, H., Tokumoto, M. & Achiba, Y. (2003), 'Near-infrared saturable absorption of single-wall carbon nanotubes prepared by laser ablation method', *Japanese Journal of Applied Physics, Part 2: Letters* 42(5 A), 494 – 496.

Satishkumar et al., 1998. Satishkumar, B., Govindaraj, A., Sen, R. & Rao, C. (1998), 'Single-walled nanotubes by the pyrolysis of acetylene-organometallic mixtures', *Chemical Physics Letters* 293(1-2), 47 – 52.

Set et al., 2004*a*. Set, S. Y., Yaguchi, H., Tanaka, Y. & Jablonski, M. (2004*a*), 'Laser mode locking using a saturable absorber incorporating carbon nanotubes', *Journal of Lightwave Technology* 22(1), 51 – 56.

Set et al., 2004*b*. Set, S. Y., Yaguchi, H., Tanaka, Y. & Jablonski, M. (2004*b*), 'Ultrafast fiber pulsed lasers incorporating carbon nanotubes', *IEEE Journal on Selected Topics in Quantum Electronics* 10(1), 137 – 146.

Song et al., 2007. Song, Y.-W., Morimune, K., Set, S. Y. & Yamashita, S. (2007), 'Polarization insensitive all-fiber mode-lockers functioned by carbon nanotubes deposited onto tapered fibers', *Applied Physics Letters* 90(2), 021101.

Yamashita et al., 2004. Yamashita, S., Inoue, Y., Maruyama, S., Murakami, Y., Yaguchi, H., Jablonski, M. & Set, S. (2004), 'Saturable absorbers incorporating carbon nanotubes directly synthesized onto substrates and fibers and their application to mode-locked fiber lasers', *Optics Letters* 29(14), 1581 – 1583.

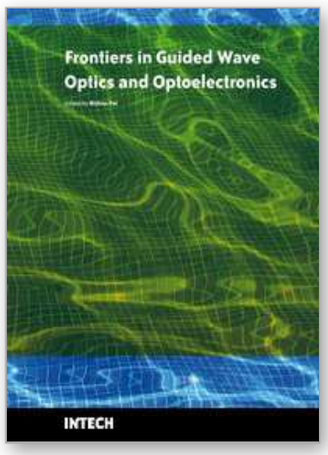

Frontiers in Guided Wave Optics and Optoelectronics

Edited by Bishnu Pal

ISBN 978-953-7619-82-4
Hard cover, 674 pages
Publisher InTech
Published online 01, February, 2010
Published in print edition February, 2010

As the editor, I feel extremely happy to present to the readers such a rich collection of chapters authored/co-authored by a large number of experts from around the world covering the broad field of guided wave optics and optoelectronics. Most of the chapters are state-of-the-art on respective topics or areas that are emerging. Several authors narrated technological challenges in a lucid manner, which was possible because of individual expertise of the authors in their own subject specialties. I have no doubt that this book will be useful to graduate students, teachers, researchers, and practicing engineers and technologists and that they would love to have it on their book shelves for ready reference at any time.

INTECH
open science | open minds

InTech Europe
University Campus STeP Ri
Slavka Krautzeka 83/A
51000 Rijeka, Croatia
Phone: +385 (51) 770 447
Fax: +385 (51) 686 166
www.intechopen.com

InTech China
Unit 405, Office Block, Hotel Equatorial Shanghai
No.65, Yan An Road (West), Shanghai, 200040, China
中国上海市延安西路65号上海国际贵都大饭店办公楼405单元
Phone: +86-21-62489820
Fax: +86-21-62489821

IntechOpen